HHS Public Access

Author manuscript

Eur J Heart Fail. Author manuscript; available in PMC 2015 November 23.

Published in final edited form as:

Eur J Heart Fail. 2014 May ; 16(5): 519–525. doi:10.1002/ejhf.73.

Diaphragm dysfunction in heart failure is accompanied by increases in neutral sphingomyelinase activity and ceramide content

Hyacinth M. Empinado[1], **Gergana M. Deevska**[2], **Mariana Nikolova-Karakashian**[2], **Jeung-Ki Yoo**[1], **Demetra D. Christou**[1], and **Leonardo F. Ferreira**[1]

[1]Department of Applied Physiology and Kinesiology, College of Health and Human Performance, University of Florida, Gainesville, FL

[2]Department of Physiology, College of Medicine, University of Kentucky, Lexington Kentucky.

Abstract

Aims—Chronic heart failure (CHF) causes inspiratory (diaphragm) muscle weakness and fatigue that contributes to dyspnoea and limited physical capacity in patients. However, the mechanisms that lead to diaphragm dysfunction in CHF remain poorly understood. Cytokines and angiotensin II are elevated in CHF and stimulate the activity of the enzyme sphingomyelinase (SMase) and accumulation of its reaction product ceramide. In the diaphragm, SMase or ceramide exposure *in vitro* causes weakness and fatigue. Thus, elevated SMase activity and ceramide content have been proposed as mediators of diaphragm dysfunction in CHF. In the present study, we tested the hypotheses that diaphragm dysfunction was accompanied by increases in diaphragm SMase activity and ceramide content.

Methods and results—We used myocardial infarction to induce CHF in rats. We measured diaphragm isometric force, SMase activity by high-performance liquid chromatography, and ceramide subspecies and total ceramide using mass spectrometry. CHF depressed diaphragm force and accelerated fatigue. Diaphragm neutral SMase activity was increased by 20% in CHF, while acid SMase activity was unchanged. We also found that CHF increased the content of C_{18}-, C_{20}, and C_{24}-ceramide subspecies and total ceramide. Downstream of ceramide degradation, diaphragm sphingosine was unchanged, and sphingosine-1-phosphate (S1P) was increased in CHF.

Conclusion—Our major novel finding was that diaphragm dysfunction in CHF rats was accompanied by higher diaphragm neutral SMase activity, which is expected to cause the observed increase in diaphragm ceramide content.

Keywords

skeletal muscle; force; sphingolipids; myocardial infarction; dyspnea

Corresponding author Leonardo F. Ferreira, PhD, Dept. Applied Physiology and Kinesiology, University of Florida, 100 FLG Stadium Rd, Gainesville, FL, 32611-8205, Phone: 352-294-1724, Fax: 352-392-5262, Ferreira@hhp.ufl.edu.

Disclosures

The authors have no conflict of interest.

Introduction

Dyspnoea and exercise intolerance are some of the most debilitating symptoms of chronic heart failure (CHF). These symptoms are determined, in part, by inspiratory (diaphragm) muscle weakness (1-3). In addition to weakness, CHF patients also experience diminished inspiratory muscle endurance that is suggestive of accelerated diaphragm fatigue (4). Abnormalities of the diaphragm can impact the ability of CHF patients to sustain increased ventilation seen at rest or during exercise (5, 6), affecting clinical management and sensation of dyspnoea (7). However, the mechanisms that could lead to diaphragm dysfunction in CHF remain poorly understood and suitable therapeutic targets have not been identified.

Inflammatory cytokines [e.g., TNF-α and interleukins (8, 9)] and angiotensin II are considered endocrine mediators of diaphragm weakness in CHF (10, 11). Cytokines and angiotensin II stimulate the activity of the enzyme sphingomyelinase (SMase) and accumulation of its reaction product ceramide (12, 13). Accordingly, serum and cardiac muscle SMase activity are increased in CHF (14, 15). In the diaphragm, SMase or ceramide exposure *in vitro* mimics the effects of CHF as seen by depressed force in diaphragm bundles and single fibres (2, 3, 16). Thus, increased SMase activity and ceramide content might be associated with diaphragm dysfunction in CHF.

In the present study, we used the myocardial infarction model of CHF in rats to test two main hypotheses: 1) CHF decreases force and accelerates fatigue of the diaphragm, and 2) CHF increases diaphragm SMase activity and ceramide content. We also examined the sphingolipid profile of the soleus muscle to test if any effects seen were unique of the diaphragm. Unveiling the effects of CHF on key components of the sphingolipid signalling pathway in the diaphragm should help identify potential mechanisms contributing to weakness and the debilitating dyspnoea experienced by patients.

Methods

Animals and surgical procedures

We used Lewis rats aged 8-10 weeks at the start of the study. Animals were housed at the University of Florida Animal Care Facilities under a 12:12 hour light and dark cycle and had access to standard chow and water *ad libitum*. All procedures were approved by the University of Florida Institutional Animal Care and Use Committee.

Rats were anesthetized using isoflurane and intubated for mechanical ventilation. We exposed the heart through a left thoracotomy and ligated the left coronary artery near the left atrium using 6-0 monofilament absorbable PGA suture (Demesorb, Demetech, USA). After ligation, the thoracic and skin incisions were closed using 3-0 PGA and nylon sutures, respectively. Sham operations mimicked the procedure for MI without ligation of the artery. Animals received topical bupivacaine and subcutaneous buprenorphine post-surgery. We performed echocardiography (see below) and terminal experiments 14-16 weeks post-surgery. On the day of the experiment, we anaesthetized the rats using isoflurane and performed a laparotomy and thoracotomy to collect blood and tissue samples. A portion of the costal diaphragm was quickly freed from adipose tissue and frozen in liquid N_2, while a

diaphragm strip was dissected for assessment of contractile function *in vitro*. The soleus was rapidly dissected and frozen in liquid N_2. The right (RV) and left ventricles (LV) were dissected for measurements of weight and infarct area by planimetry.

Echocardiography

All images were recorded with rats under 2% isoflurane anesthesia. Two-dimensional M-mode ultrasound images were obtained at 7.5 MHz (Toshiba Aplio) in the parasternal long- and short-axis view. We determined left ventricle (LV) end-diastolic diameter (LVEDD), LV end-systolic diameter (LVESD), LV posterior wall thickness during diastole (LVPWThD) and systole (LVPWThS), and LV posterior wall shortening velocity (LVPWSV) over five cardiac cycles. Measurements were performed using the leading edge-to-leading edge method. LV fractional shortening (FS) was calculated using the formula %FS = (LVEDD − LVESD) × 100/(LVEDD).

Diaphragm contractile properties

The procedure used for assessment of diaphragm isometric force is similar to that described previously (16, 17). Briefly, a diaphragm muscle strip was dissected and placed at optimal length for twitch force production (L_0). Isometric contractile characteristics were measured at 37°C using a Dual-Mode Muscle Lever System (300C-LR, Aurora Scientific Inc, Aurora, Canada) while the muscle was stimulated supramaximally using a biphasic high-power stimulator (701C, Aurora Scientific Inc.). Stimulus frequencies ranged from 1 to 200 Hz (0.25 ms pulse and 0.5 s train durations) in solution containing D-tubocurarine (25 μM). Five minutes after the force-frequency stimulations, we determined isometric fatigue properties using a protocol consisting of 40 Hz stimulus, 500 ms train, and 0.5 trains per second (16). We analysed the force-frequency relationship from each animal using a four-parameter Hill equation to define the shape of the curve. For fatigue characteristics, we measured peak forces during the 1^{st}, 25^{th}, 50^{th}, 75^{th} and 100^{th} contraction of the protocol. Forces were normalized to peak value during the 1^{st} contraction to determine fatigue.

Myosin heavy chain gel electrophoresis

To determine whether the effects of CHF on diaphragm fatigue could be accompanied by changes in diaphragm fibre type composition, we used MHC gel electrophoresis (18). We identified types I, and IIa/IIx isoforms of MHC. Our gels did not yield resolution to separate IIa/IIx isoforms as these have very similar molecular weights. Thus, we analysed and report a combined percentage of IIa/IIx isoforms.

Sphingomyelinase activity assays

Serum SMase, A-SMase and N-SMase activities were measured using C6-NBD-SM as a substrate. Serum samples were used as the source of S-SMase. The standardized assay contained serum (2 μl), 20 μM NBD-SM, 0.1 mM $ZnCl_2$, 0.1 M sodium acetate buffer (pH 5.0) in a final volume of 20 μl. In parallel, assays were done in Zn-free buffer containing EDTA to account for any activity associated with cell debris or other contaminants in the serum sample. The S-SMase activity was calculated as the difference of the activity in the presence and absence of Zn. A-SMase and N-SMase activities were measured in diaphragm

homogenates prepared in 10 mM Tris-HCl, pH 7.4, 1 mM EDTA, 1 mM sodium orthovanadate, 15 mM sodium fluoride and protease inhibitor cocktail (Sigma-Aldrich). Protein concentrations were assessed with a Lowry total protein determination kit (DC Protein Assay; BioRad, Hercules, CA), and 40 μg were used in each assay. The N-SMase activity assay was done in a 50 mM Tris-HCl (pH 7.4) reaction buffer containing 7.5 mM $MgCl_2$, 10 μM C6-NBD-SM, 1 mM sodium ortovanadate, 15 mM sodium fluoride, protease inhibitor cocktail and 40 μg of homogenate in a final volume of 40 μl for 30 min. The A-SMase activity assay was done in 100 mM sodium acetate buffer, (pH 4.5) containing 0.2 mM β-mercaptoethanol, 10 μM C6-NBD-SM, 1 mM sodium ortovanadate, 15 mM sodium fluoride, protease inhibitor cocktail and 40μg of homogenate in a final volume of 40μl for 3 h. For all three types of assays, reactions were stopped by the addition of 0.5 ml methanol. After further incubation at 37°C for 30 min, the samples were centrifuged at 1,000 × g, and the clear supernatant was transferred to clear HPLC vials. The generation of fluorescent product, NBD-ceramide was monitored by a reverse phase HPLC using methanol:water:phosphoric acid (850:150:0.15, by vol.) as a mobile phase (19).

Sphingolipid content

Muscles were homogenized in 1X TGS buffer (Bio-Rad, Hercules, CA). Aliquots of the lysate were shipped on dry ice to the Lipidomics Core at the Medical University of South Carolina for extraction and analysis of sphingolipid content by tandem mass spectrometry using a TSQ 7000 triple quadrupole mass spectrometer (Thermo-Fisher Scientific, Waltham, MA) as described previously (20).

RNA isolation, cDNA synthesis and qRT-PCR

Rat diaphragm (~50 mg) was homogenized in Trizol Reagent (Life Techonologies, Grand Island, NY) according to the manufacturer's instructions using a Kinematica Polytron PT-2100 Homogenizer (Kinematica, Bohemia, NY). RNA concentrations were measured and cDNA was synthesized from 1 μg RNA using the RETROscript Kit (Life Techonologies, Carlsbad, CA) according to the manufacturer's instructions. Real-time polymerase chain reactions were ran using an ABI Prism 7000 Sequence Detection System with primers and probes for for ASMase (Smpd1), N-SMase2 (Smpd3), N-SMase3 (Smpd4), sphingosine kinase 1 (Sphk1), S1P lyase (Sgpl1), S1P phosphatase 1 (Spp1), and the housekeeping gene 18S RNA (Life Technologies, Carlsbad, CA). The probes for all genes consisted of a Taqman 5′-FAM labeled reporters and 3′-nonfluorescent quenchers.

Western blots

The procedures used to determine protein abundance have been described in detail in a recent study (21). Briefly, we loaded proteins onto a 4-15% criterion pre-cast gel, run, and transferred to a low-fluorescence PVDF membrane (Immobilon-FL, Millipore). We blocked membranes in 5% milk and exposed the membrane to primary antibodies for sphingosine kinase 1 (Cell Signaling) and α-tubulin (DSHB, University of Iowa, Iowa City, IA) at 1:1000. Secondary antibodies were fluorescence-conjugated IRDye (Li-COR, Lincoln, Nebraska). Membranes were scanned using Odyssey Imager using two-channel detection and analyzed using Image Studio Lite (Li-COR).

Statistical analysis

We used commercially available software for statistical analyses (Prism 5.0b, GraphPad Software Inc., La Jolla, CA and SigmaPlot, Systat Software). In general, comparisons between groups were performed by t-test or the Mann-Whitney test when data did not pass a normalcy test. Fatigue and ceramide subspecies data were analysed by ANOVA as detailed in the results sections. Data are shown as mean ± SE unless stated otherwise. Differences were considered statistically significant when $P < 0.05$.

Results

The 14-16 week survival rate was 78% in the coronary artery ligation group. One rat that underwent MI surgery had a left ventricle with a small infarct size (< 10% LV area) and normal FS and, therefore, was not included in our studies. The characteristics of animals in each group are shown in Table 1. Tissue weights and echocardiography variables showed typical signs of heart failure in infarcted rats.

Diaphragm contractile function

We observed that diaphragm twitch and maximal tetanic forces were decreased in our CHF rats (Fig. 1). Twitch kinetics were similar between groups as noted by unchanged time to peak tension (in ms; Sham 18.5 ± 1.3, CHF 18.7 ± 1.0) and ½ relaxation time (in ms; Sham 21.6 ± 1.6, CHF 21.8 ± 2.3). Accordingly, the frequency that elicited 50% of maximal response (in Hz; Sham 43 ± 0.7 Hz, CHF 43 ± 0.9 Hz) and the slope of the sigmoid (Hill coefficient; Sham 3.4 ± 0.1, CHF 3.2 ± 0.1) were unaltered in CHF. These results suggest a uniform decrease in muscle force across all frequencies. During the fatigue protocol, peak force during the first contraction was lower in CHF (10.3 ± 0.4 N/cm^2) than Sham (12.1 ± 0.5 N/cm^2). Regardless, decrements in normalized force (% initial) were more pronounced in CHF diaphragm after 25 and 50 contractions. The faster fatigue could not be explained by changes in MHC isoforms of the diaphragm due to CHF (Fig. 1C).

Sphingomyelinase activity

We measured the activity of the three SMases that may affect cellular ceramide content via sphingomyelin (SM) hydrolysis. In the diaphragm muscle, we observed that the activity of N-SMase was increased by ~20% in CHF while acid SMase activity was unchanged (Fig. 2). The activity of SMase measured in serum was decreased in CHF (in nmol/ml/hr: Sham, 11.9 ± 0.7 and CHF, 10.1 ± 0.50; $P < 0.05$).

Muscle sphingolipid content

The major diaphragm ceramide species were C_{18}-, C_{20}- and C_{24}-ceramide and were substantially increased in rats with CHF (Fig. 3A), resulting in an elevation of approximately 20% in total ceramide content (Fig. 3B). Other less-abundant ceramide species were similar in the diaphragms of control and CHF rats. Notably, the mass-spec analysis identified a series of rare ceramide species (Fig. 3A; inset) with short, very long, or highly unsaturated fatty acids, i.e., arachidonic acid. These rare species were not affected by CHF. Similarly, the levels of sphingosine were unchanged (Fig. 3C), but the levels of S1P,

which is produced by phosphorylation of sphingosine by sphingosine kinase-catalysed reaction were increased 2-fold (Fig. 3D).

In the soleus muscle, C_{18}- and C_{20}-ceramide were increased in CHF (Table 2). However, this was not a consistent response among subspecies such that CHF did not increase total soleus ceramide levels. No changes in sphingosine were present in the soleus muscle (Table 2), while S1P levels tended to be decreased by CHF ($P < 0.10$).

Sphingolipid metabolizing enzymes: mRNA and protein abundance

The elevated N-SMase activity, ceramide, and S1P content in the diaphragm could be due to increased gene expression or post-translational modification of proteins involved in sphingolipid metabolism. Our measurements of mRNA and protein expression revealed unchanged abundance of SMases that convert sphingomyelin to ceramide (Fig. 4). CHF seemed to decrease the mRNA abundance of sphingosine kinase 1 (SK1). We then tested SK1 protein abundance and found it to be decreased by CHF (Fig.4B). The mRNA levels of S1P lyase and S1P phosphatase 1 (SPP1) were unchanged in CHF, with similar results for S1P lyase protein abundance while we could not detect SPP1 in our Western Blots (data not shown).

Discussion

Our major novel finding was that diaphragm weakness and fatigue in CHF rats was accompanied by higher diaphragm neutral SMase activity and increased content of C_{18}-, C_{20}-, and C_{24}-ceramide subspecies and total ceramide. CHF effects on skeletal muscle sphingolipid profile were not ubiquitous as the soleus did not show a response entirely consistent with the diaphragm.

Diaphragm weakness and fatigue in CHF

Our finding of diaphragm weakness in CHF is in agreement with previous studies in animals and humans (1, 2, 4). An important observation of our study was that CHF accelerated diaphragm fatigue *in vitro*. This suggests that alterations intrinsic to the diaphragm muscle cells contribute to the diminished respiratory muscle endurance seen in CHF patients (4). Diaphragm fibre type composition was similar in control and CHF rats. In humans, there is unchanged (22) or slightly increase type I fibre composition in CHF diaphragm (23). Our findings suggest that contractile dysfunction, and not a fibre type shift, contributes to diaphragm fatigue. Among the mechanisms proposed for weakness and fatigue in CHF are cytokines (10), angiotensin II (24), oxidants (25), and increased SMase activity (12, 14) or accumulation of ceramide (16).

Sphingolipid signalling cascade in CHF diaphragm dysfunction

Doehner et al. (14) reported increased serum SMase activity in CHF patients, while we found lower serum SMase activity in CHF rats. Data from a recent study in patients is also consistent with our observations (26). The reasons for these potential discrepancies are unclear at present, but data from one study suggests that myocardial infarction elicits time-dependent changes in serum SMase activity (27).

Neutral SMase activity was increased in the diaphragm of CHF rats. Based on unchanged gene expression of diaphragm SMases, we consider that post-translational modifications activate SMase in CHF (e.g., oxidation or phosphorylation) (12). For example, TNF-α (8) and oxidative stress (25) are elevated in CHF and could be responsible for activation of N-SMase in the diaphragm (12). The increased diaphragm N-SMase activity in CHF is expected to elevate ceramide and metabolites downstream of ceramide. Accordingly, CHF increased ceramide content ~20%. These changes in ceramide are of similar magnitude to those elicited by high fat diet, where muscle ceramide contributes to vascular dysfunction and insulin resistance (28, 29). Thus, the accumulation of ceramide that we observed can be sufficient to cause diaphragm dysfunction in CHF. In support of this idea, exposure of diaphragm bundles to SMase or ceramide *in vitro* depresses maximal force and accelerates fatigue (16, 17). Overall, the general effects of SMase and ceramide on diaphragm are similar to those elicited by CHF: increased oxidants, weakness, and accelerated fatigue [Fig. 1 and refs. (2, 25)].

Establishing causality and clinical relevance

Our study identifies increased N-SMase activity and ceramide content as plausible mediators and therapeutic targets against diaphragm weakness and fatigue in CHF. However, a major challenge to establish causality is that specific inhibitors of N-SMase appropriate for *in vivo* studies are not yet available (30), and knockouts animals of neutral SMase are either unsuitable for CHF studies or unavailable (31). If new therapies targeted to increased N-SMase activity and ceramide are developed and yield positive results in CHF diaphragm function, it would be clinically relevant.

Cardiac rehabilitation is a key component of the integrated clinical management of CHF (32). The importance of inspiratory muscle weakness is evident from the beneficial effects of inspiratory muscle training added to standard cardiac rehabilitation for these patients (7, 33). Based on outcomes of inspiratory muscle training studies, the benefits of treating diaphragm weakness pharmacologically are expected to have a positive impact on the clinical management and quality of life of CHF patients.

In conclusion, diaphragm muscle from CHF rats are weaker and fatigue faster than Sham controls. This diaphragm dysfunction is accompanied by increases neutral SMase activity and ceramide content in the diaphragm. The contractile and metabolic changes elicited by CHF in the diaphragm could not be explained by shifts in fibre type composition. Overall, our findings are consistent with the idea that increased N-SMase activity and ceramide content are potential candidates and therapeutic targets for diaphragm dysfunction in CHF.

Acknowledgements

We would like to thank Bumsoo Ahn, Adam Beharry, and Dr. Andrew Judge for technical assistance.

Grants

This study was supported by NIH grants to L.F. Ferreira (K99/R00-HL098453) and M. Nikolova-Karakashian (R01-AG019223). G.M. Deevska was supported by an American Heart Association postdoctoral fellowship (11POST7650060).

References

1. Meyer FJ, Borst MM, Zugck C, Kirschke A, Schellberg D, Kubler W, Haass M. Respiratory muscle dysfunction in congestive heart failure: clinical correlation and prognostic significance. Circulation. May 1; 2001 103(17):2153–8. [PubMed: 11331255]
2. van Hees HW, van der Heijden HF, Hafmans T, Ennen L, Heunks LM, Verheugt FW, Dekhuijzen PN. Impaired isotonic contractility and structural abnormalities in the diaphragm of congestive heart failure rats. Int J Cardiol. Aug 29; 2008 128(3):326–35. [PubMed: 17689734]
3. van Hees HW, van der Heijden HF, Ottenheijm CA, Heunks LM, Pigmans CJ, Verheugt FW, Brouwer RM, Dekhuijzen PN. Diaphragm single-fibre weakness and loss of myosin in congestive heart failure rats. Am J Physiol Heart Circ Physiol. Jul; 2007 293(1):H819–28. [PubMed: 17449557]
4. Dall'ago P, Chiappa GR, Guths H, Stein R, Ribeiro JP. Inspiratory muscle training in patients with heart failure and inspiratory muscle weakness: a randomized trial. J Am Coll Cardiol. 2006; 47(4): 757–63. [PubMed: 16487841]
5. Del Rio R, Marcus NJ, Schultz HD. Inhibition of hydrogen sulfide restores normal breathing stability and improves autonomic control during experimental heart failure. J Appl Physiol (1985). May; 2013 114(9):1141–50. [PubMed: 23449938]
6. Olson TP, Joyner MJ, Eisenach JH, Curry TB, Johnson BD. Influence of Locomotor Muscle Afferent Inhibition on the Ventilatory Response to Exercise in Heart Failure. Exp Physiol. Nov 29.2013
7. Cahalin LP, Arena R, Guazzi M, Myers J, Cipriano G, Chiappa G, Lavie CJ, Forman DE. Inspiratory muscle training in heart disease and heart failure: a review of the literature with a focus on method of training and outcomes. Expert Rev Cardiovasc Ther. Feb; 2013 11(2):161–77. [PubMed: 23405838]
8. Nymo SH, Hulthe J, Ueland T, McMurray J, Wikstrand J, Askevold ET, Yndestad A, Gullestad L, Aukrust P. Inflammatory cytokines in chronic heart failure: interleukin-8 is associated with adverse outcome. Results from CORONA. Eur J Heart Fail. Aug 4; 2014 16(1):68–75. [PubMed: 23918775]
9. Gielen S, Adams V, Linke A, Erbs S, Mobius-Winkler S, Schubert A, Schuler G, Hambrecht R. Exercise training in chronic heart failure: correlation between reduced local inflammation and improved oxidative capacity in the skeletal muscle. Eur J Cardiovasc Prev Rehabil. 2005; 12(4): 393–400. [PubMed: 16079649]
10. Mangner N, Linke A, Oberbach A, Kullnick Y, Gielen S, Sandri M, Hoellriegel R, Matsumoto Y, Schuler G, Adams V. Exercise training prevents TNF-alpha induced loss of force in the diaphragm of mice. PLoS One. 2013; 8(1):e52274. [PubMed: 23300968]
11. Rezk BM, Yoshida T, Semprun-Prieto L, Higashi Y, Sukhanov S, Delafontaine P. Angiotensin II infusion induces marked diaphragmatic skeletal muscle atrophy. PLoS One. 2012; 7(1):e30276. [PubMed: 22276172]
12. Nikolova-Karakashian MN, Reid MB. Sphingolipid Metabolism, Oxidant Signaling, and Contractile Function of Skeletal Muscle. Antioxid Redox Signal. Jun 8.2011
13. Berry C, Touyz R, Dominiczak AF, Webb RC, Johns DG. Angiotensin receptors: signaling, vascular pathophysiology, and interactions with ceramide. Am J Physiol Heart Circ Physiol. Dec; 2001 281(6):H2337–65. [PubMed: 11709400]
14. Doehner W, Bunck AC, Rauchhaus M, von Haehling S, Brunkhorst FM, Cicoira M, Tschope C, Ponikowski P, Claus RA, Anker SD. Secretory sphingomyelinase is upregulated in chronic heart failure: a second messenger system of immune activation relates to body composition, muscular functional capacity, and peripheral blood flow. Eur Heart J. Apr; 2007 28(7):821–8. [PubMed: 17353227]
15. Adamy C, Mulder P, Khouzami L, Andrieu-abadie N, Defer N, Candiani G, Pavoine C, Caramelle P, Souktani R, Le Corvoisier P, Perier M, Kirsch M, Damy T, Berdeaux A, Levade T, Thuillez C, Hittinger L, Pecker F. Neutral sphingomyelinase inhibition participates to the benefits of N-acetylcysteine treatment in post-myocardial infarction failing heart rats. J Mol Cell Cardiol. Sep; 2007 43(3):344–53. [PubMed: 17707397]

16. Ferreira LF, Moylan JS, Gilliam LA, Smith JD, Nikolova-Karakashian M, Reid MB. Sphingomyelinase stimulates oxidant signaling to weaken skeletal muscle and promote fatigue. Am J Physiol Cell Physiol. Sep; 2010 299(3):C552–60. [PubMed: 20519448]

17. Ferreira LF, Moylan JS, Stasko S, Smith JD, Campbell KS, Reid MB. Sphingomyelinase depresses force and calcium sensitivity of the contractile apparatus in mouse diaphragm muscle fibres. J Appl Physiol. Feb 23; 2012 112(9):1538–45. [PubMed: 22362402]

18. Tikunov BA, Sweeney HL, Rome LC. Quantitative electrophoretic analysis of myosin heavy chains in single muscle fibres. J Appl Physiol (1985). May; 2001 90(5):1927–35. [PubMed: 11299287]

19. Nikolova-Karakashian M, Morgan ET, Alexander C, Liotta DC, Merrill AH Jr. Bimodal regulation of ceramidase by interleukin-1beta. Implications for the regulation of cytochrome p450 2C11. J Biol Chem. Jul 25; 1997 272(30):18718–24. [PubMed: 9228043]

20. Bielawski J, Pierce JS, Snider J, Rembiesa B, Szulc ZM, Bielawska A. Sphingolipid analysis by high performance liquid chromatography-tandem mass spectrometry (HPLC-MS/MS). Adv Exp Med Biol. 2010; 688:46–59. [PubMed: 20919645]

21. Ahn B, Empinado HM, Al-Rajhi M, Judge AR, Ferreira LF. Diaphragm atrophy and contractile dysfunction in a murine model of pulmonary hypertension. PLoS One. 2013; 8(4):e62702. [PubMed: 23614054]

22. Lindsay DC, Lovegrove CA, Dunn MJ, Bennett JG, Pepper JR, Yacoub MH, Poole-Wilson PA. Histological abnormalities of muscle from limb, thorax and diaphragm in chronic heart failure. Eur Heart J. Aug; 1996 17(8):1239–50. [PubMed: 8869866]

23. Tikunov BA, Mancini D, Levine S. Changes in myofibrillar protein composition of human diaphragm elicited by congestive heart failure. J Mol Cell Cardiol. Dec; 1996 28(12):2537–41. [PubMed: 9004169]

24. Dalla Libera L, Ravara B, Angelini A, Rossini K, Sandri M, Thiene G, Battista Ambrosio G, Vescovo G. Beneficial effects on skeletal muscle of the angiotensin II type 1 receptor blocker irbesartan in experimental heart failure. Circulation. May 1; 2001 103(17):2195–200. [PubMed: 11331262]

25. Supinski GS, Callahan LA. Diaphragmatic free radical generation increases in an animal model of heart failure. J Appl Physiol. 2005; 99(3):1078–84. [PubMed: 16103520]

26. Knapp M, Baranowski M, Lisowska A, Musial W. Decreased free sphingoid base concentration in the plasma of patients with chronic systolic heart failure. Adv Med Sci. Jun 1; 2012 57(1):100–5. [PubMed: 22296975]

27. Knapp M, Zendzian-Piotrowska M, Blachnio-Zabielska A, Zabielski P, Kurek K, Gorski J. Myocardial infarction differentially alters sphingolipid levels in plasma, erythrocytes and platelets of the rat. Basic Res Cardiol. Nov.2012 107(6):294. [PubMed: 22961594]

28. Zhang QJ, Holland WL, Wilson L, Tanner JM, Kearns D, Cahoon JM, Pettey D, Losee J, Duncan B, Gale D, Kowalski CA, Deeter N, Nichols A, Deesing M, Arrant C, Ruan T, Boehme C, McCamey DR, Rou J, Ambal K, Narra KK, Summers SA, Abel ED, Symons JD. Ceramide mediates vascular dysfunction in diet-induced obesity by PP2A-mediated dephosphorylation of the eNOS-Akt complex. Diabetes. Jul; 2012 61(7):1848–59. [PubMed: 22586587]

29. Bikman BT, Guan Y, Shui G, Siddique MM, Holland WL, Kim JY, Fabrias G, Wenk MR, Summers SA. Fenretinide prevents lipid-induced insulin resistance by blocking ceramide biosynthesis. J Biol Chem. May 18; 2012 287(21):17426–37. [PubMed: 22474281]

30. Canals D, Perry DM, Jenkins RW, Hannun YA. Drug targeting of sphingolipid metabolism: sphingomyelinases and ceramidases. Br J Pharmacol. Jun; 2011 163(4):694–712. [PubMed: 21615386]

31. Stoffel W, Jenke B, Block B, Zumbansen M, Koebke J. Neutral sphingomyelinase 2 (smpd3) in the control of postnatal growth and development. Proc Natl Acad Sci U S A. Mar 22; 2005 102(12): 4554–9. [PubMed: 15764706]

32. McMurray JJ, Adamopoulos S, Anker SD, Auricchio A, Bohm M, Dickstein K, Falk V, Filippatos G, Fonseca C, Gomez-Sanchez MA, Jaarsma T, Kober L, Lip GY, Maggioni AP, Parkhomenko A, Pieske BM, Popescu BA, Ronnevik PK, Rutten FH, Schwitter J, Seferovic P, Stepinska J, Trindade PT, Voors AA, Zannad F, Zeiher A, Bax JJ, Baumgartner H, Ceconi C, Dean V, Deaton

C, Fagard R, Funck-Brentano C, Hasdai D, Hoes A, Kirchhof P, Knuuti J, Kolh P, McDonagh T, Moulin C, Reiner Z, Sechtem U, Sirnes PA, Tendera M, Torbicki A, Vahanian A, Windecker S, Bonet LA, Avraamides P, Ben Lamin HA, Brignole M, Coca A, Cowburn P, Dargie H, Elliott P, Flachskampf FA, Guida GF, Hardman S, Iung B, Merkely B, Mueller C, Nanas JN, Nielsen OW, Orn S, Parissis JT, Ponikowski P. ESC guidelines for the diagnosis and treatment of acute and chronic heart failure 2012: The Task Force for the Diagnosis and Treatment of Acute and Chronic Heart Failure 2012 of the European Society of Cardiology. Developed in collaboration with the Heart Failure Association (HFA) of the ESC. Eur J Heart Fail. Aug; 2012 14(8):803–69. [PubMed: 22828712]

33. Marco E, Ramirez-Sarmiento AL, Coloma A, Sartor M, Comin-Colet J, Vila J, Enjuanes C, Bruguera J, Escalada F, Gea J, Orozco-Levi M. High-intensity vs. sham inspiratory muscle training in patients with chronic heart failure: a prospective randomized trial. Eur J Heart Fail. Aug; 2013 15(8):892–901. [PubMed: 23512093]
34. Danieli-Betto D, Peron S, Germinario E, Zanin M, Sorci G, Franzoso S, Sandona D, Betto R. Sphingosine 1-phosphate signaling is involved in skeletal muscle regeneration. Am J Physiol Cell Physiol. Mar; 2010 298(3):C550–8. [PubMed: 20042733]
35. Danieli-Betto D, Germinario E, Esposito A, Megighian A, Midrio M, Ravara B, Damiani E, Libera LD, Sabbadini RA, Betto R. Sphingosine 1-phosphate protects mouse extensor digitorum longus skeletal muscle during fatigue. Am J Physiol Cell Physiol. Jun; 2005 288(6):C1367–73. [PubMed: 15659717]
36. Meissner A, Yang J, Kroetsch JT, Sauve M, Dax H, Momen A, Noyan-Ashraf MH, Heximer S, Husain M, Lidington D, Bolz SS. Tumor necrosis factor-alpha-mediated downregulation of the cystic fibrosis transmembrane conductance regulator drives pathological sphingosine-1-phosphate signaling in a mouse model of heart failure. Circulation. Jun 5; 2012 125(22):2739–50. [PubMed: 22534621]

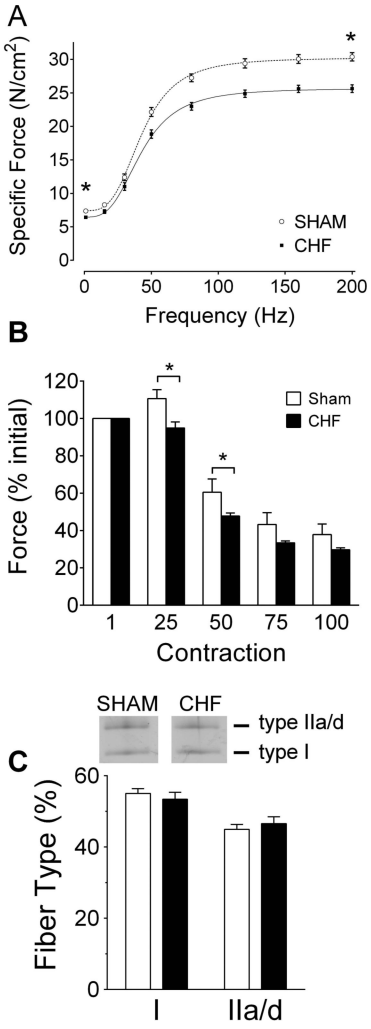

Figure 1.

Diaphragm weakness and fatigue in rats with chronic heart failure (CHF). **A**) Force-frequency relationship. Specific force, force normalized for bundle cross sectional area. Data are mean ± SE from Sham (n = 10) and CHF (n = 13) rats. Twitch (1 Hz) and maximal tetanic (200 Hz) forces were lower in CHF rats (* $P < 0.05$, t-test). Dotted and solid lines are line of best fit of mean data using Hill equation. **B**) Diaphragm fatigue during submaximal tetanic contractions. Forces are normalized within each animal to percentage of peak value for the first contraction during the fatigue protocol. The increase in normalized force seen in Sham after 25 contractions reflect post-tetanic potentiation. Data are mean ± SE for Sham (n = 5) and CHF rats (n = 8). * $P < 0.05$ for Sham vs. CHF (repeated measures ANOVA and Tukey's post-hoc test). **C)** Diaphragm fibre type composition based on myosin heavy chain (MHC) isoforms determined by SDS-PAGE. Images are representative profile of MHC in gels. Data are mean ± SE from n = 5 animals per group.

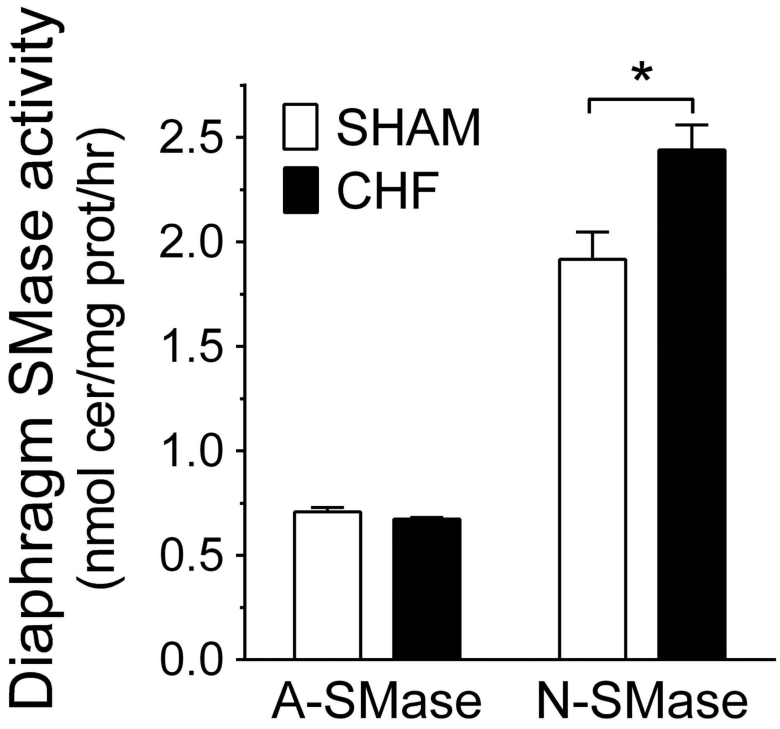

Figure 2.

Heart failure increases diaphragm sphingomyelinase (SMase) activity. A-SMase, acid sphingomyelinase; N-SMase, neutral sphingomyelinase. **A**) Measurements of enzyme activity were made in whole-tissue homogenates. Data are shown in nmol ceramide/mg protein/hour for Sham (n = 7) and CHF (n = 10) rats. All values are expressed as mean ± SE. **P* < 0.05 by t-test.

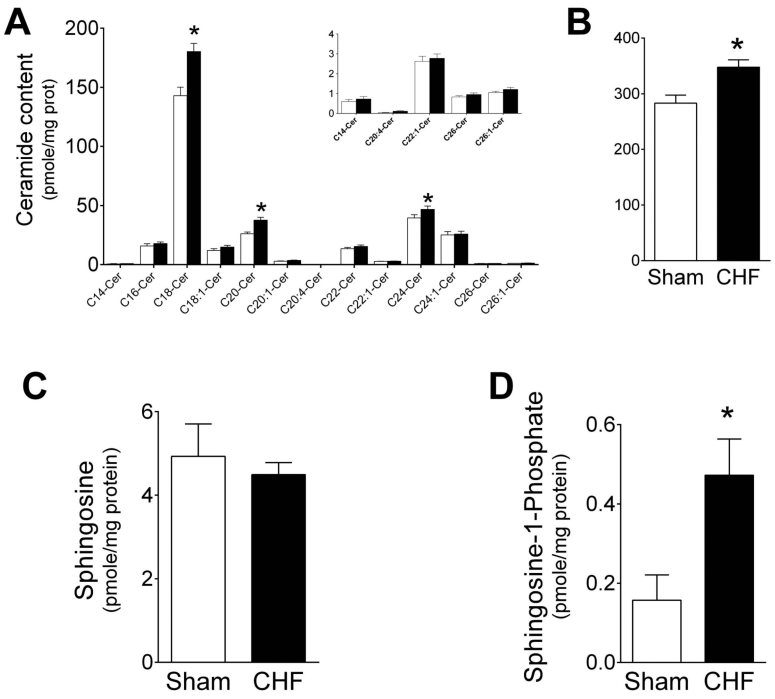

Figure 3.

Heart failure increases diaphragm ceramide content. **A**) Content of each ceramide subspecies measured in rat diaphragm. *Inset*, data from select ceramide subspecies shown in different scale for clarity of visualization. Open bars, Sham (n = 16); closed bars, CHF (n = 21). **B**) Total ceramide content calculated as the sum of individual subspecies shown in panel A. * $P < 0.05$ by ANOVA and Bonferroni post-hoc test for planned comparison (Panel A) and t-test (Panel B) **C**) Sphingosine content. **D**) Sphingosine-1-phosphate content. Data from one Sham animal (2.28 pmole/mg protein) was identified as an outlier by Grubb's test and was not included in graph and statistical analysis shown above. * $P < 0.005$ by Mann-Whitney test. In healthy skeletal muscle, S1P promotes growth and regeneration (34, 35). In CHF, elevation of S1P in vascular smooth muscle causes vasoconstriction (36).

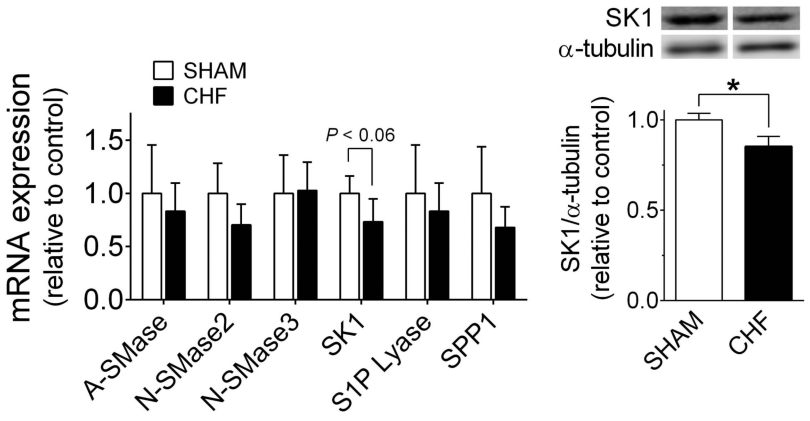

Figure 4.

Diaphragm expression of select sphingolipid metabolizing enzymes. **A)** Relative mRNA abundance of sphingomyelinases, acid (A-SMase) and neutral (N-SMase) isoforms, sphingosine kinase 1 (SK1), sphingosine-1-phosphaste (S1P) lyase, and S1P phosphatase 1 (SPP1). Data are from n = 5 rats per group. **B)** Protein abundance of SK1 is diminished in CHF diaphragm. Data are normalized to α-tubulin (loading control) and expressed as mean ± SE. * $P < 0.05$ by t-test

Table 1

Animal characteristics and echocardiographic variables

	Sham	CHF
Infarct area (%)	-	25 ± 2
Body weight (initial, g)	254 ± 6	258 ± 4
Body weight (final, g)	415 ± 4	427 ± 5
LV wt/TL (mg/mm)	18 ± 0.6	21 ± 0.6*
RV wt/TL (mg/mm)	4.0 ± 0.2	5.1 ± 0.2*
Lung wt/TL (mg/mm)	26 ± 0.5	27 ± 0.7
LVEDD (mm)	7.6 ± 0.1	8.6 ± 0.2*
LVESD (mm)	4.2 ± 0.1	5.9 ± 0.1*
FS (%)	44 ± 1	32 ± 1*
LVPWThD (mm)	1.59 ± 0.03	1.40 ± 0.04*
LVPWThS (mm)	2.57 ± 0.05	2.25 ± 0.07
LVPWSV (mm/s)	35 ± 1	29 ± 1*
HR (beats/min)	382 ± 5	361 ± 6*

LV, left ventricle; RV, right ventricle; TL, tibial length; LVEDD, LV end-diastolic diameter; LVESD, LV end-systolic diameter; LVPWTh, LV posterior wall thickness during diastole (D) and systole (S); LVPWSV, posterior wall shortening velocity; FS, fractional shortening; HR, heart rate.

*$P < 0.05$ by t-test for Sham (n = 18) vs. CHF (n = 22).

Table 2

Sphingolipid content in soleus muscle.

	Sham	CHF
C_{14}-cer	0.20 ± 0.10	0.23 ± 0.07
C_{16}-cer	22 ± 3	16.9 ± 1.4
C_{18}-cer	46 ± 4	61 ± 5.5*
$C_{18:1}$-cer	2.6 ± 0.2	3.0 ± 0.2
C_{20}-cer	23 ± 2.7	30 ± 3.1*
$C_{20:1}$-cer	1.5 ± 0.2	1.8 ± 0.2
C_{22}-cer	8.0 ± 1.0	8.5 ± 0.5
$C_{22:1}$-cer	1.4 ± 0.2	1.3 ± 0.1
C_{24}-cer	28 ± 3.2	31 ± 2.3
$C_{24:1}$-cer	17 ± 2.3	15 ± 0.9
C_{26}-cer	0.17 ± 0.10	0.24 ± 0.07
$C_{26:1}$-cer	0.41 ± 0.09	0.44 ± 0.09
Total ceramide	150 ± 14	170 ± 11
Sphingosine	2.6 ± 0.44	2.3 ± 0.05
S1P	0.45 ± 0.14	0.17 ± 0.08

Ceramide (cer) subspecies identified in soleus muscle using mass spectrometry in sham (n = 6) and CHF rats (n = 8). Total ceramide is the sum of all subspecies detected herein. S1P, sphingosine-1-phosphate. Data are mean ± SE and expressed in in pmol/mg prot.

*P < 0.05 by ANOVA and Bonferroni post-hoc analysis.